Supporting information

Water compatible synthesis of 1,2,3-triazoles under ultrasonic conditions by a Cu(I) complex-mediated click reaction

Juan-Carlos Castillo,[a,b] Nestor-Fabian Bravo,[a] Lenka-Victoria Tamayo,[c] Paula-Daniela Mestizo,[c] John Hurtado,[c,]* Mario Macías,[d] and Jaime Portilla[a,]*

[a] *Bioorganic Compounds Research Group, Department of Chemistry, Universidad de los Andes, Carrera 1 No. 18A-10, 111711 Bogotá, Colombia*

[b] *Escuela de Ciencias Química, Universidad Pedagógica y Tecnológica de Colombia, Avenida Central del Norte 39-115, Tunja 150003, Colombia*

[c] *Grupo de Investigación en Química Inorgánica, Catálisis y Bioinorgánica, Department of Chemistry, Universidad de los Andes, Carrera 1 No. 18A-10, Bogotá, 111711, Colombia.*

[d] *Department of Chemistry, Universidad de los Andes, Carrera 1 No. 18A-10, Bogotá, 111711, Colombia.*

*Email: jportill@uniandes.edu.co; jj.hurtado@uniandes.edu.co

Contents

1. Overview of substrates and products numbering

Benzyl halides and analogous **1a–e** and ligand **7**

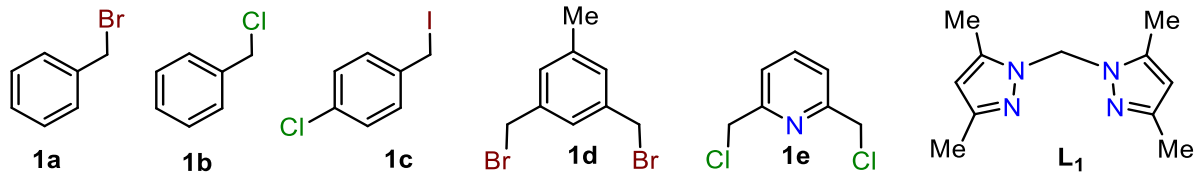

Terminal alkynes **3a–h**

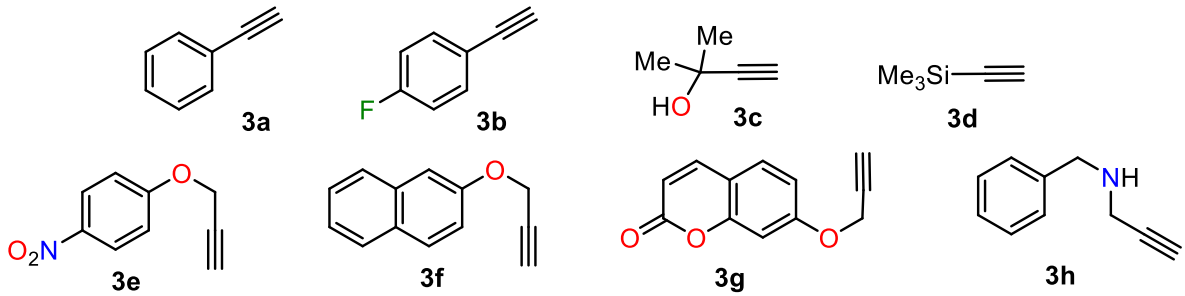

1,4-Disubstituted 1,2,3-triazoles **4a–l**

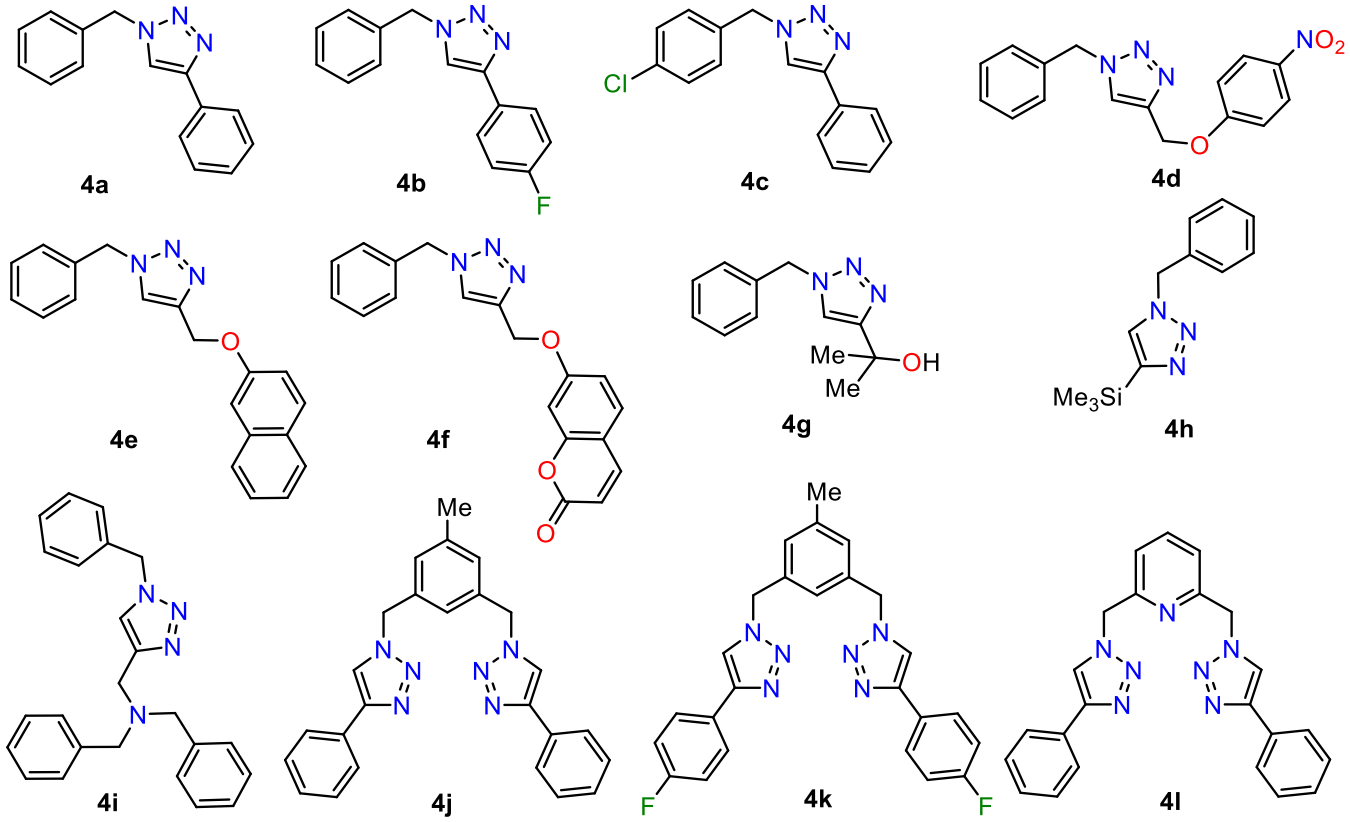

Scheme S1. Structure of all substrates intermediates and products involved in this research

2. General scheme for the synthesis of this research

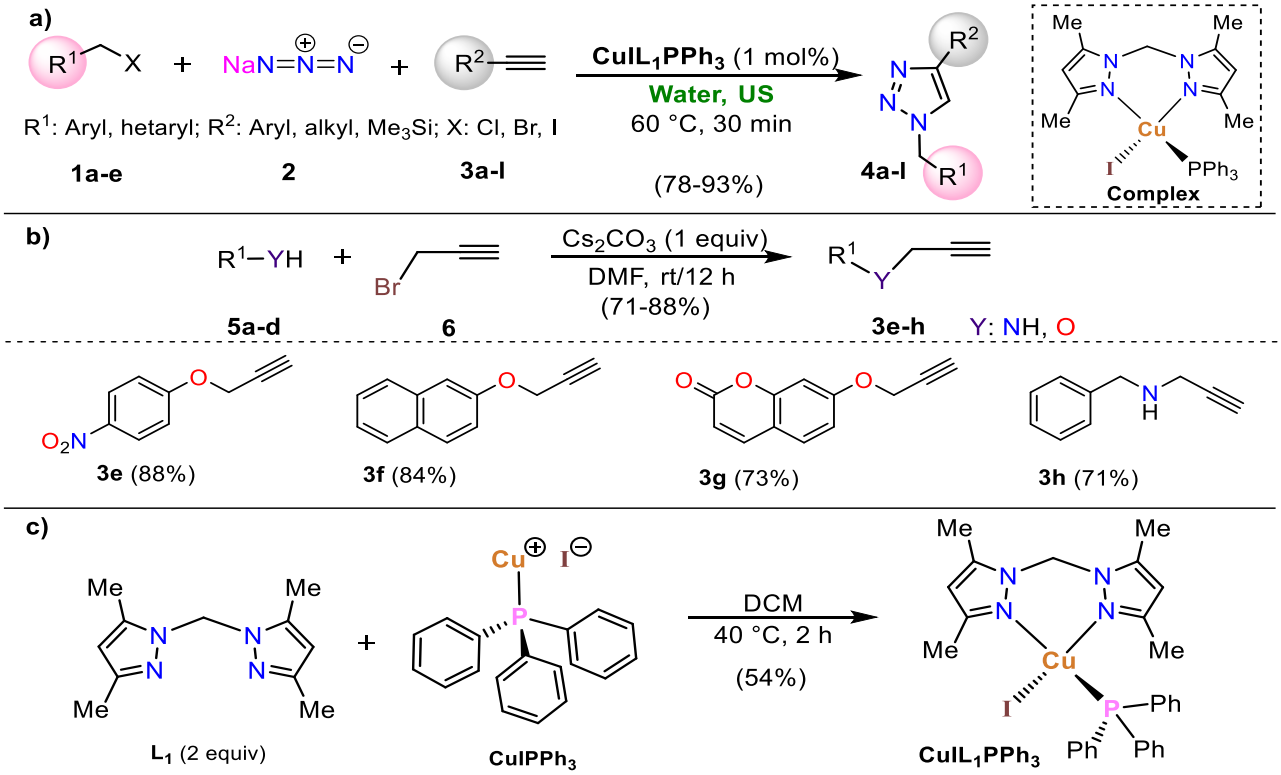

Scheme S2 Synthesis of a) 1,2,3-triazoles **4a–l**, b) alkynes **3e–h** and c) **CuL₁PPh₃** complex

3. FTIR and RAMAN spectra of complex

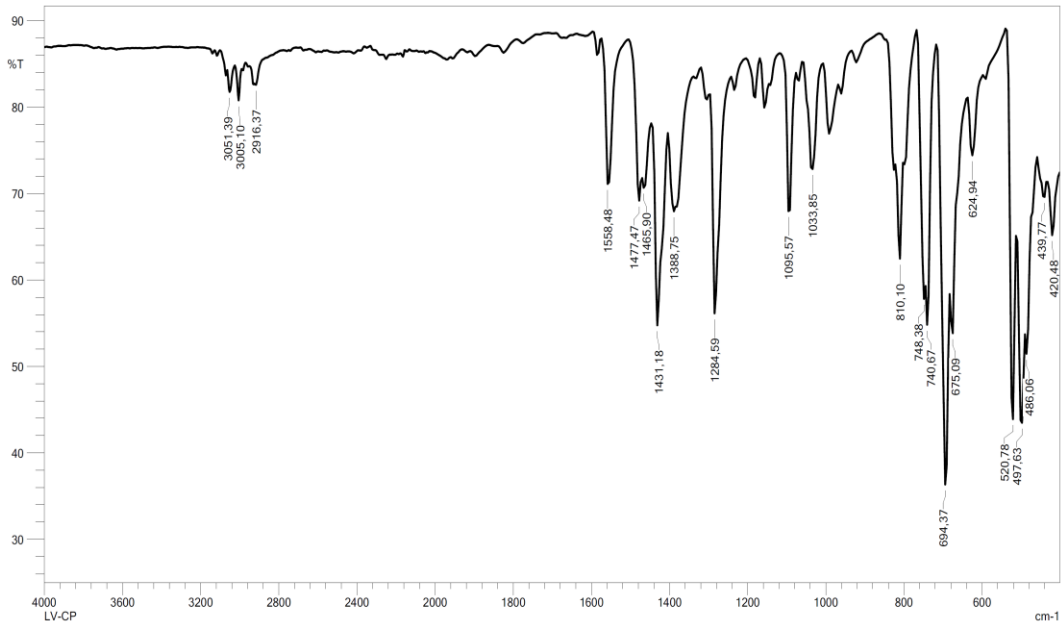

Figure S1. FTIR spectrum of **CuIL₁PPh₃** complex

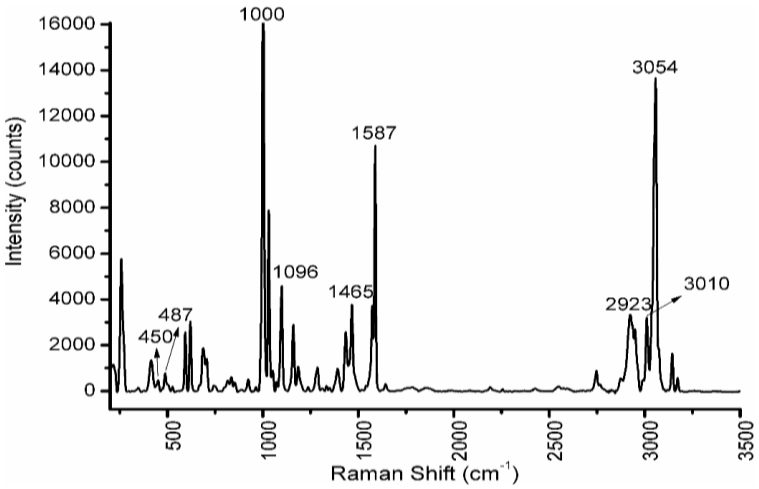

Figure S2. Raman spectrum of **CuIL$_1$PPh$_3$** complex

4. Crystallographic details of CuIL$_1$PPh$_3$ complex

Complexes **8** and **CuIL$_1$PPh$_3$** were recrystallized via slow evaporation procedure from a solution of acetonitrile and were mounted in oil. The data collection and refinement details are summarized in Table S1. In the refinements, all the non-hydrogen atoms were anisotropically treated, and the hydrogen atoms were generated geometrically, placed in the calculated positions (C–H = 0.93–0.97 Å) and included as riding contributions with isotropic displacement parameters set at 1.2–1.5 times the U_{eq} value of the parent atom. The final refinement for **8** shows values related to residual nonmodelled electron density in the solvent accessible voids. The low average quality of the crystals obtained for this compound does not allow an appropriate refinement of the solvent. Therefore, the SQUEEZE utility[1] in PLATON[2] was used to model its contribution to the overall intensity data.

4.1. Comments

Complex [CuIPPh$_3$]$_4$ crystallizes in the Monoclinic *I*2/*c* space group forming molecules with a central backbone-like structure constituted of Cu and I atoms building a finite ladder (Fig. S3a).[3a] This sort of molecular structure was also observed in the coordination polymer $C_{10}H_6CuIN_3O$ which crystallized as a helical structure with the Cu and I atoms forming an infinite ladder.b[3b] The copper cations present two independent coordination geometries with the Cu(2) describing tetrahedral coordination bonded to one threephenylphosfine (PPh$_3$) group and three iodine atoms with an average volume of 8.747 Å^3 and a mean quadratic elongation of λ = 1.014.[4] Cu(1) has an infrequent distorted trigonal planar

geometry bonded to one PPh_3 group and two iodine atoms. This tricoordinate copper was also observed in other molecules such as the Cu(I) complex with *bis*(phosphino)borate ligands, Cu(I) amido and aminyl radical complexes and copper (II) aryls.[5–7] The Cu···Cu distance, with a value of 2.87 Å, is not too far from the sum of the van der Waals radii (2.8 Å), implying a probable metal-metal bonding interaction. The structure has a Z´value of 0.5, which is due to the coincident symmetry of the molecule with an inversion center at (1/2, 1/2, 1/2). The intermolecular assembly in crystal is mainly controlled by dispersion and other van der Waals forces considering that no classic hydrogen bonds were found.

Table S1. Selected crystallographic data for complexes **$[CuIPPh_3]_4$** and **$CuIL_1PPh_3$**

Crystal data	**$[CuIPPh_3]_4$**	**$CuIL_1PPh_3$**
Chemical formula	$C_{72}H_{60}Cu_4I_4P_4$	$C_{29}H_{31}CuIN_4P$
M_r	1810.88	657.00
Crystal system, space group	Monoclinic, *I*2/*c*	Triclinic, *P*-1
a, *b*, *c* (Å)	18.3661 (16), 16.0719 (14), 27.117 (3)	10.7747 (8), 15.4475 (10), 19.6421 (12)
α, β, γ (°)	90.0, 108.602 (10), 90.0	109.743 (6), 99.759 (5), 103.575 (6)
V (Å^3)	7586.2 (13)	2878.4 (4)
Z	4	4
μ (mm^{-1})	2.86	1.91
Crystal size (mm)	0.30 × 0.13 × 0.10	0.31 × 0.14 × 0.12
Data collection		
T_{min}, T_{max}	0.332, 1.000	0.865, 1.000
No. of measured, independent and observed [$I > 2\sigma(I)$] reflections	38232, 8330, 6399	59943, 12529, 8524
R_{int}	0.064	0.088
$(\sin \theta/\lambda)_{max}$ (Å^{-1})	0.641	0.641
Refinement		
$R[F^2 > 2\sigma(F^2)]$, $wR(F^2)$, S	0.039, 0.105, 1.03	0.052, 0.156, 1.10
No. of reflections	8330	12529
No. of parameters	434	657
$\Delta\rho_{max}$, $\Delta\rho_{min}$ (e Å^{-3})	0.83, −0.71	1.14, −0.95

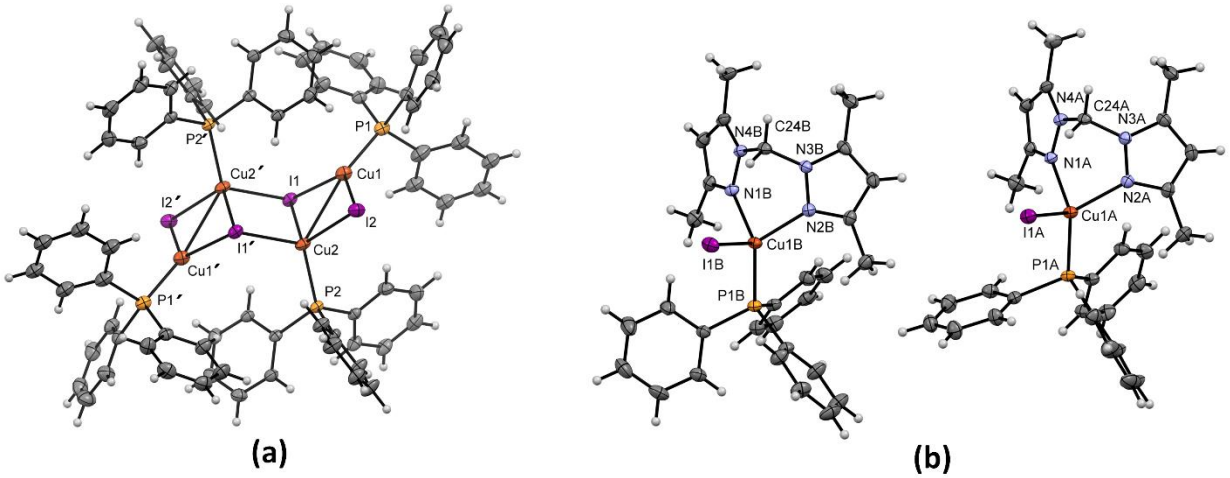

Figure S3. Structure of (a) **[CuIPPh$_3$]$_4$** and (b) two independent molecules of **CuIL$_1$PPh$_3$** complex, showing the anisotropic displacement ellipsoids drawn at the 20% probability level. H atoms are shown as small spheres of arbitrary radii. Only relevant atoms are labeled for the sake of clarity.

The new **CuIL$_1$PPh$_3$** complex crystallizes in the Triclinic *P*-1 space group forming two independent molecules in the asymmetric unit with different conformations observed in the level of rotation of the phenyl rings in the PPh_3 group (Figure S3b). The molecular structure is conformed by the complexation of one *bis*(3,5-dimethyl-1*H*-pyrazol-1-yl)methane (**L$_1$**) ligand, one PPh_3 ligand and one iodine atom coordinating the central copper cation, that is, a complexes of mononuclear nature. The copper has tetrahedral coordination with an average volume of 5.727 Å^3 and a mean quadratic elongation of λ = 1.058.[4] The chelate rings from the ligand **L$_1$** in molecules A and B adopt a boat conformation with the Cu1(A,B) and C24(A,B) atoms deviated to the same side of the main plane and puckering parameters Q = 0.825(3) Å/θ = 88.9(2) °/φ = 6.7(2) ° and Q = 0.803(3) Å/θ = 90.4(2) °/φ = 9.4(3) (2) ° for A and B, respectively. This conformation was also observed in other complexes showing that this structural tendency is kept despite the differences in the coordination number and the length of the coordinated bonds.[8–12] Similarly to complex 1, the supramolecular structure is dominated by dispersion and van der Waals forces since no classic hydrogen bonds were found. In general, both complexes ([CuIPPh$_3$]$_4$ and **CuIL$_1$PPh$_3$**) were synthesized as molecular systems with very similar Cu–P distances with values of ~2.2 Å and Cu–I lengths have values between 2.5 Å-2.7 Å, which is in agreement with those observed in the double-stranded copper(I) helicate $C_{10}H_6CuIN_3O$.[3] Selected bond lengths (Å) and bond angles (°) for both compounds are summarized in Table S2.

The energy levels of the Frontier Molecular Orbitals (FMOs) HOMO (highest occupied molecular orbital) and LUMO (lowest unoccupied molecular orbital) for the studied complexes [CuIPPh$_3$]$_4$ and

$CuIL_1PPh_3$ were computed (Figure S4). These calculations were carried out through the STO-3G basis set at the Hartree–Fock level of theory implemented in *CrystalExplorer*[13] using the crystallographic information files (.cif) obtained from the X-ray diffraction measurements. These FMOs are the main orbital participating in chemical reactions and they are also used for predicting the most reactive position in diverse molecular systems. For example, the HOMO energy describes the ability of electron-donor orbitals while the LUMO describes the ability of electron-acceptor, and the energy gap between HOMO and LUMO could describes the hardness and softness of a molecular complex. Interactions between harder chemical entities (larger the HOMO-LUMO gap values) are more likely to be dominated by electrostatic interactions, such as in the tricomponent click reaction in water Cu(I) mediated presented in this work.[14]

Table S2 Selected bond lengths (Å) and bond angles (°) for complexes **$[CuIPPh_3]_4$** and **$CuIL_1PPh_3$**

Complex 8					
I1–Cu1	2.5823(8)	Cu1–I1–Cu2	65.48(2)	I1–Cu2–I2	109.42(2)
I1–Cu2	2.7203(7)	Cu1–I1–Cu2´	104.63(2)	I1–Cu2–P2	113.82(4)
I1–Cu2´	2.7253(7)	Cu2–I1–Cu2´	79.46(2)	I1–Cu2–I1´	100.54(2)
I2–Cu1	2.5357(7)	Cu1–I2–Cu2	67.23(2)	I2–Cu2–P2	112.71(3)
I2–Cu2	2.6466(8)	I1–Cu1–I2	117.73(3)	I2–Cu2–I1´	103.73(2)
Cu1–P1	2.2301(13)	I1–Cu1–P1	114.17(4)	P2–Cu2–I1´	115.54(4)
Cu2–P2	2.2425(10)	I2–Cu1–P1	126.71(4)		
Complex $CuIL_1PPh_3$: Molecules A/B					
I1–Cu1	2.7175(7)/ 2.6922(7)	I1–Cu1–P1	107.85(4)/ 110.28(4)	P1–Cu1–N1	122.42(10)/ 119.24(10)
Cu1–P1	2.2101(11)/ 2.2026(12)	I1–Cu1–N1	108.07(9)/ 105.86(9)	P1–Cu1–N2	123.09(10)/ 124.09(10)
Cu1–N1	2.088(3)/ 2.121(3)	I1–Cu1–N2	103.78(9)/ 103.67(10)	N1–Cu1–N2	89.22(13)/ 90.91(13)
Cu1–N2	2.123(3)/ 2.072(3)				

In $[CuIPPh_3]_4$, the HOMO almost exhibits no metal character and it is located at two equatorial phenyl groups, whereas the LUMO is found to possess a good metal character, and it is located mainly around the Cu(I) atoms and over two axial PPh_3 groups of $[CuIPPh_3]_4$. The relatively high magnitude (poor hardness) of the HOMO-LUMO energy gap (2.56 eV) explains the poor charge transfer interactions taking place within the molecule $[CuIPPh_3]_4$ (poor softness) (Figure S4a). Regarding complex **$CuIL_1PPh_3$**, the FMOs are localized at the whole molecular complex (except the methylene group,

CH_2). In this case, the HOMO displays a good metal character but it is mostly located at both ligands (**L_1** and PPh_3), whereas the LUMO is found to possess a very strong metal character mostly located around the Cu(I) atom (Figure S4b). The high magnitude (strong hardness) of the energy separation between the HOMO and LUMO (7.14 eV) apparently help explain the high catalytic power of this homonuclear complex in the click reaction studied by us, which is governed by both electrostatic interactions and steric effects (Figure S4).

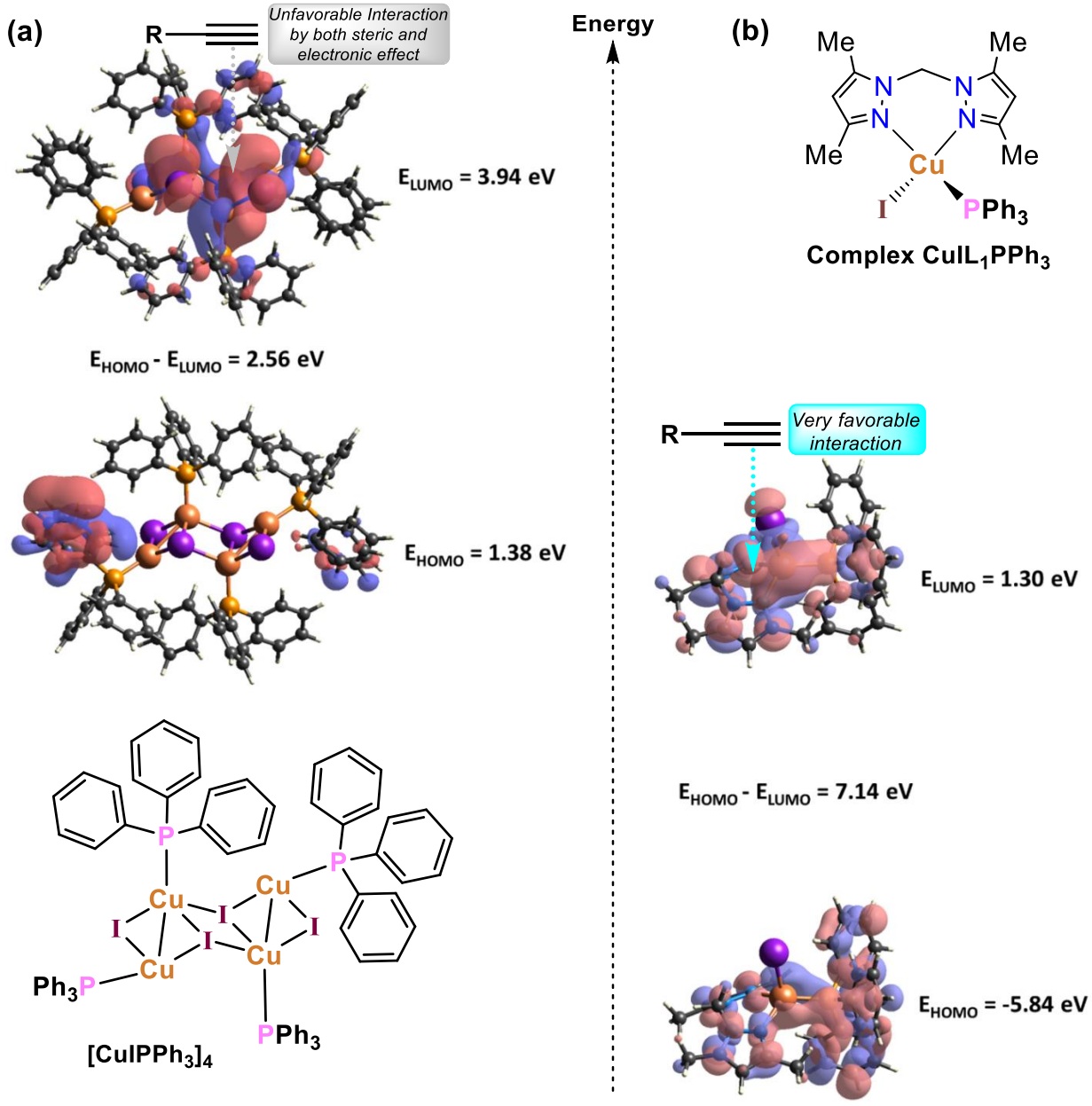

Figure S4. Computed energy levels HOMO–LUMO for complexes (a) **$[CuIPPh_3]_4$** and (b) **$CuIL_1PPh_3$** using the crystallographic information files (.cif) by STO-3G basis set at the Hartree–Fock level theory.

5. Copies of NMR spectra

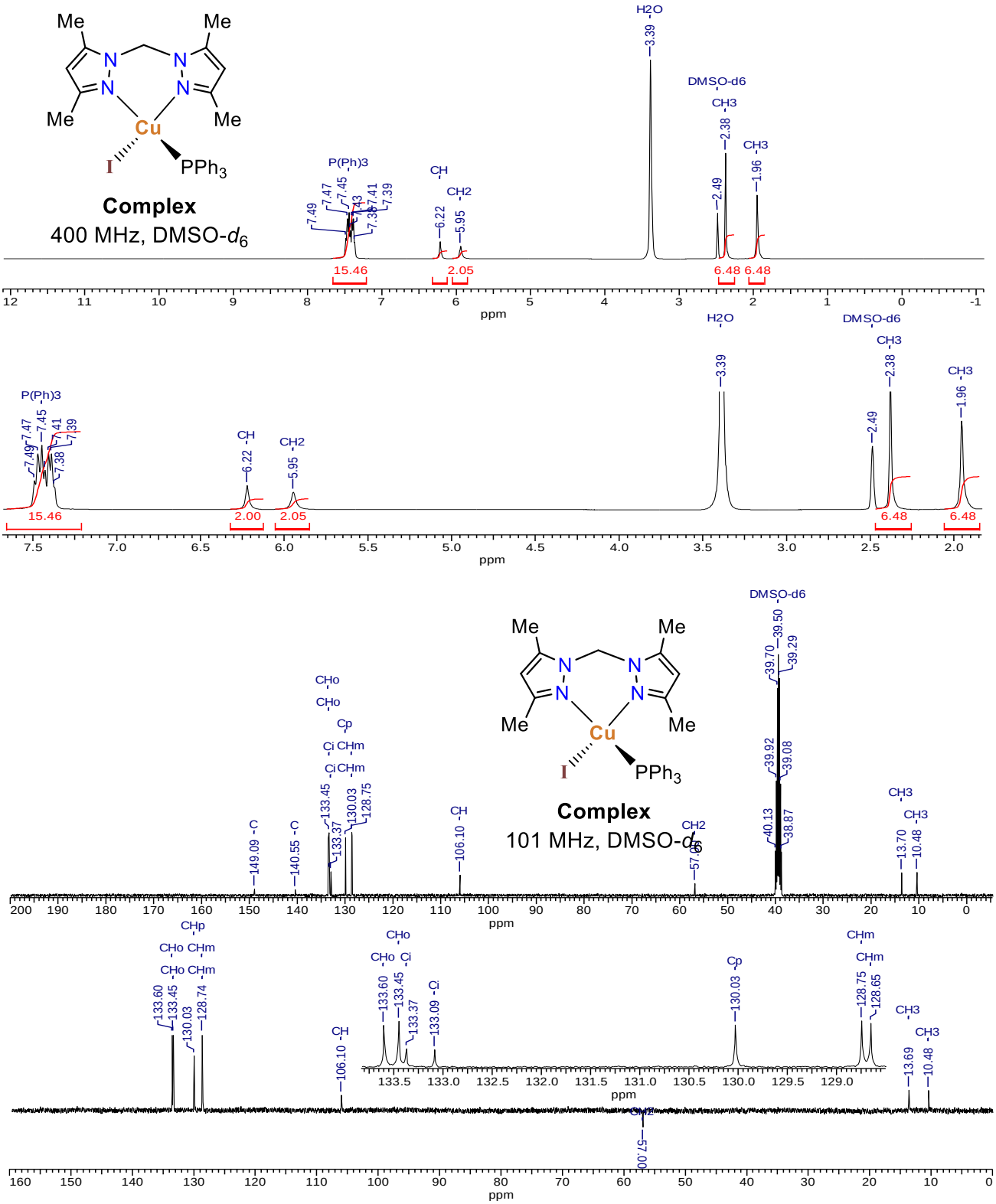

Figure S5. ^{1}H and $^{13}C\{^{1}H\}$ NMR spectra of **$CuIL_1PPh_3$** complex

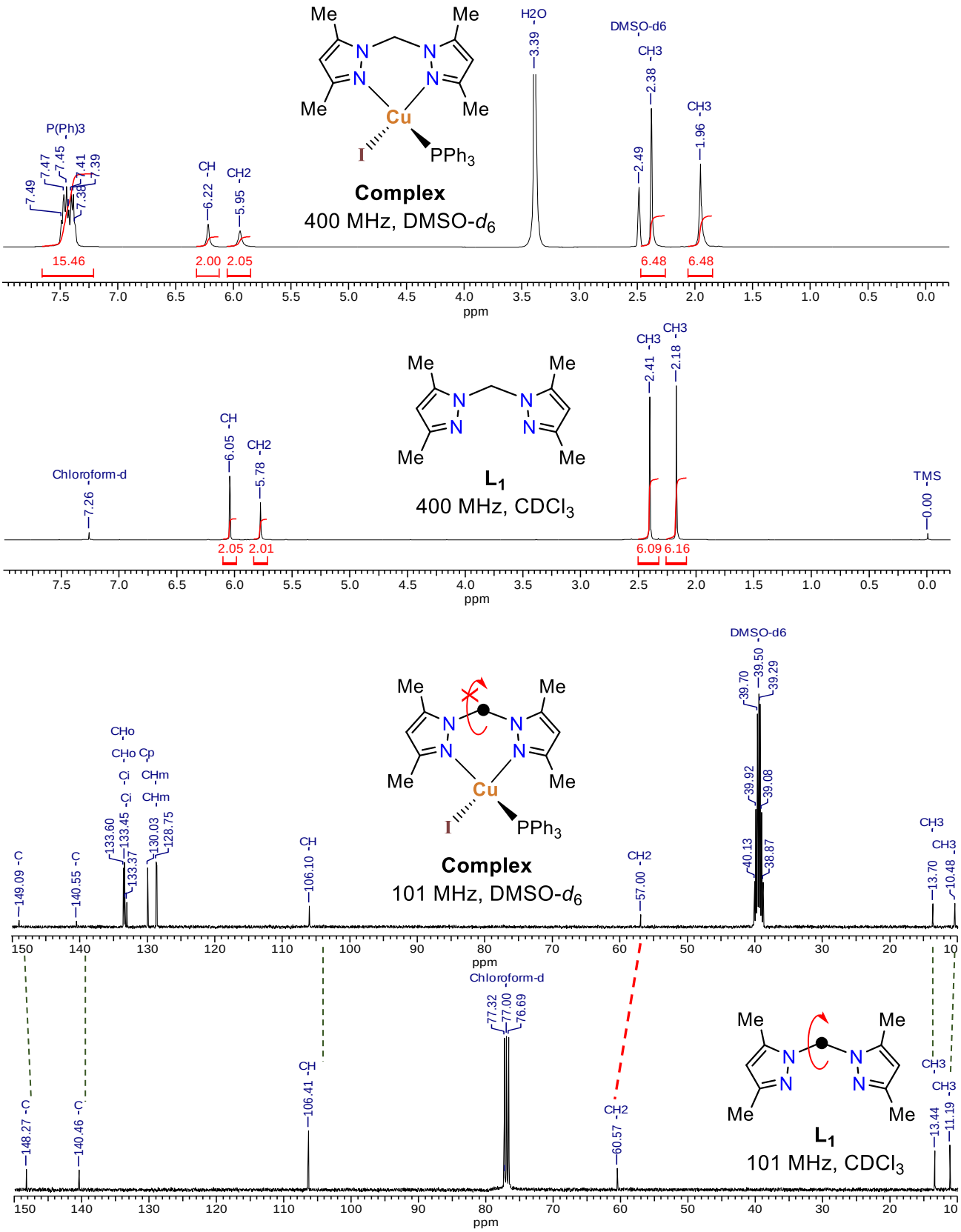

Figure S6. ^{1}H and $^{13}C\{^{1}H\}$ NMR spectra of **CuIL$_1$PPh$_3$** complex *versus* ligand **L$_1$**

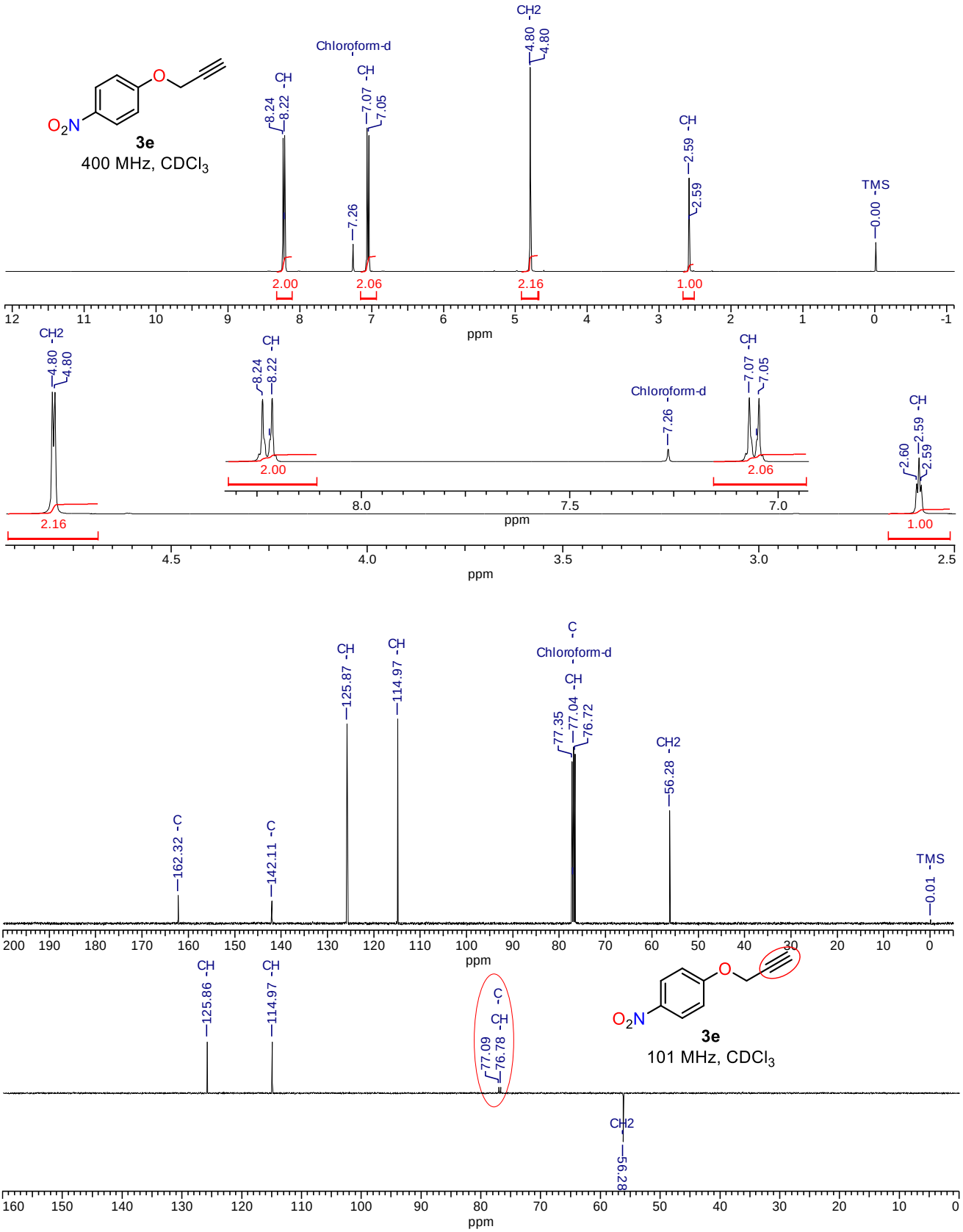

Figure S7. ^{1}H and $^{13}C\{^{1}H\}$ NMR spectra of 1-nitro-4-(prop-2-yn-1-yloxy)benzene (**3e**)

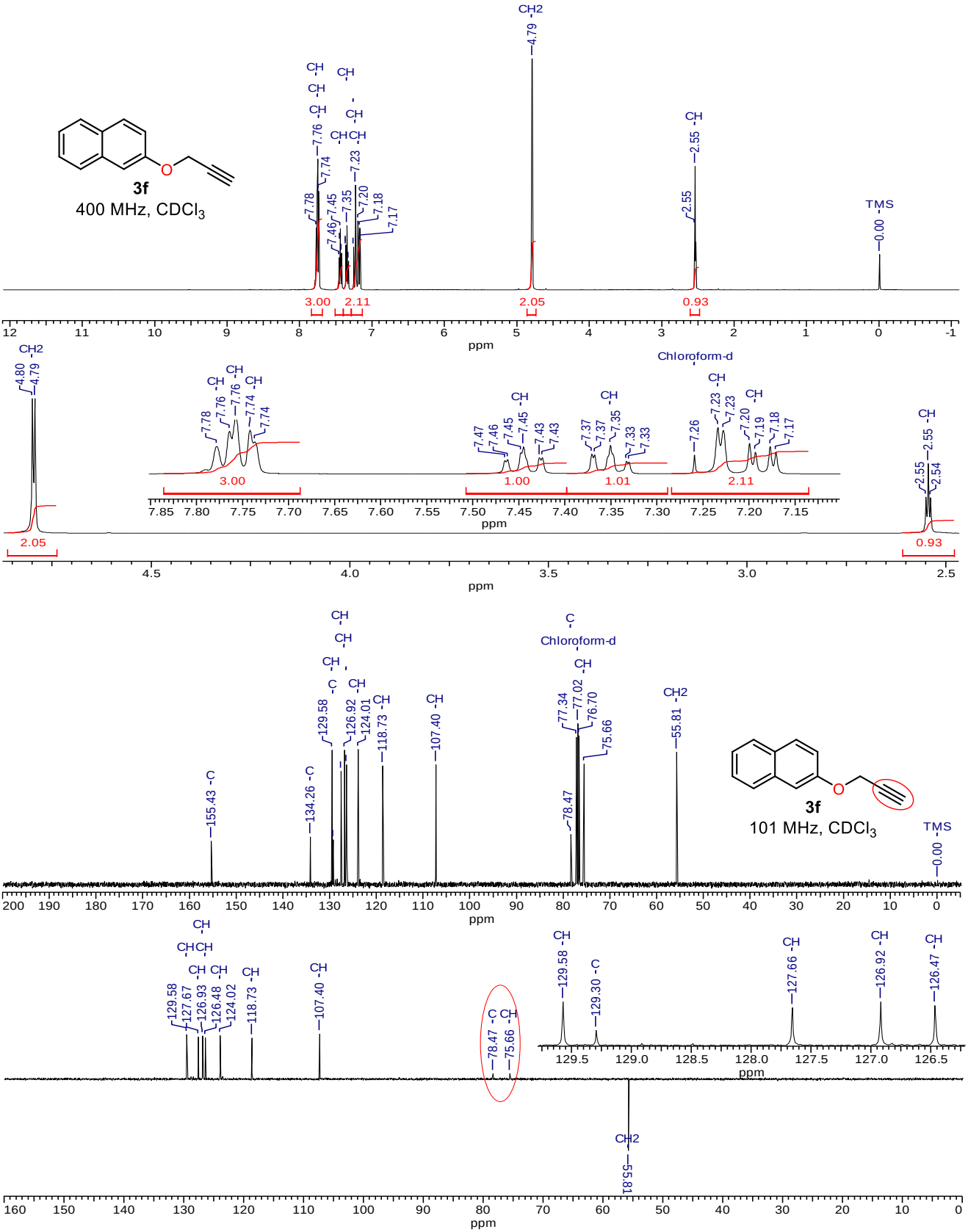

Figure S8. ^{1}H and $^{13}C\{^{1}H\}$ NMR spectra of 2-(prop-2-yn-1-yloxy)naphthalene (**3f**)

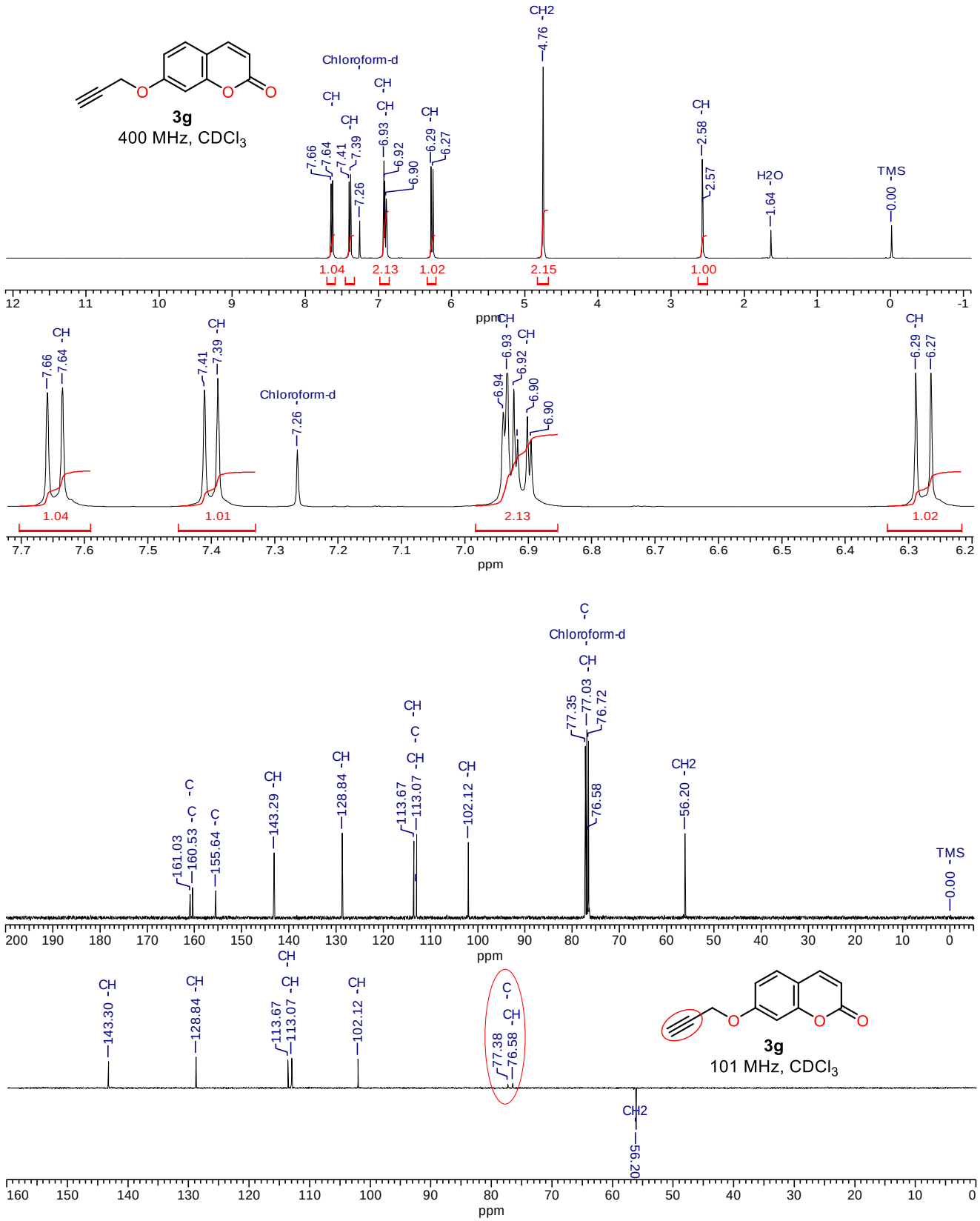

Figure S9. ^{1}H and $^{13}C\{^{1}H\}$ NMR spectra of 7-(prop-2-yn-1-yloxy)-2*H*-chromen-2-one (**3g**)

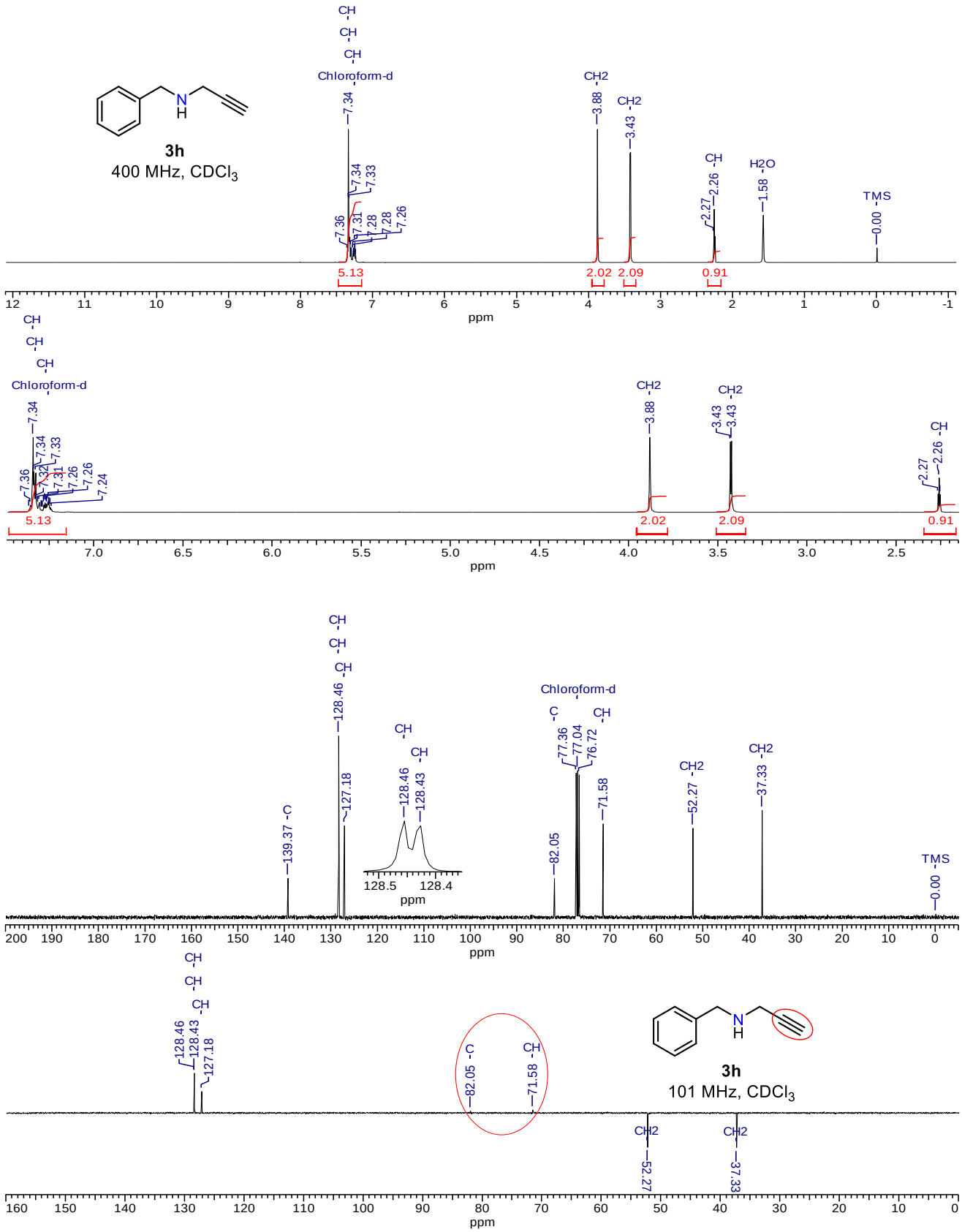

Figure S10. ^{1}H and $^{13}C\{^{1}H\}$ NMR spectra of *N*-benzylprop-2-yn-1-amine (**3g**)

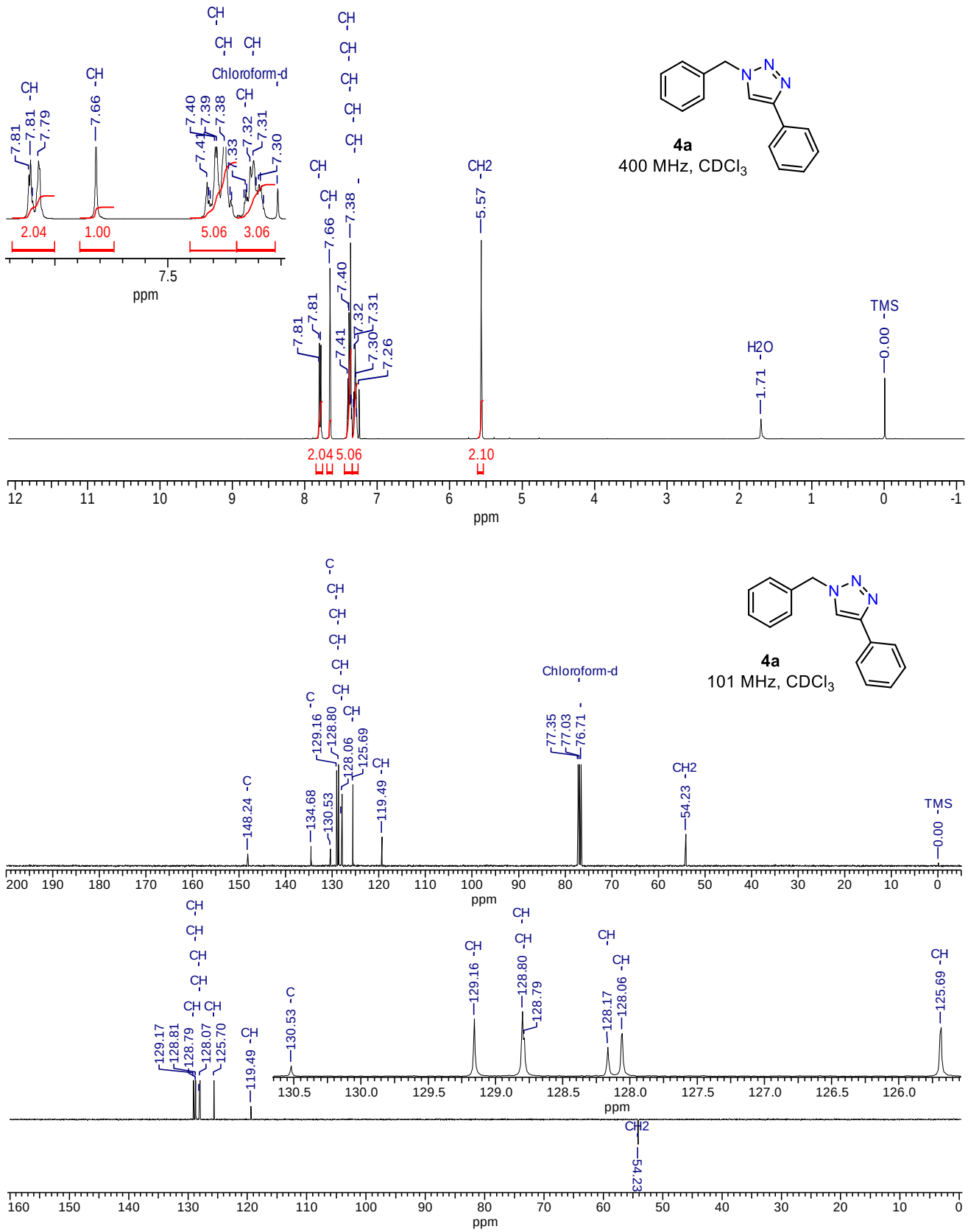

Figure S11. ^{1}H and $^{13}C\{^{1}H\}$ NMR spectra of 1-benzyl-4-phenyl-1*H*-1,2,3-triazole (**4a**)

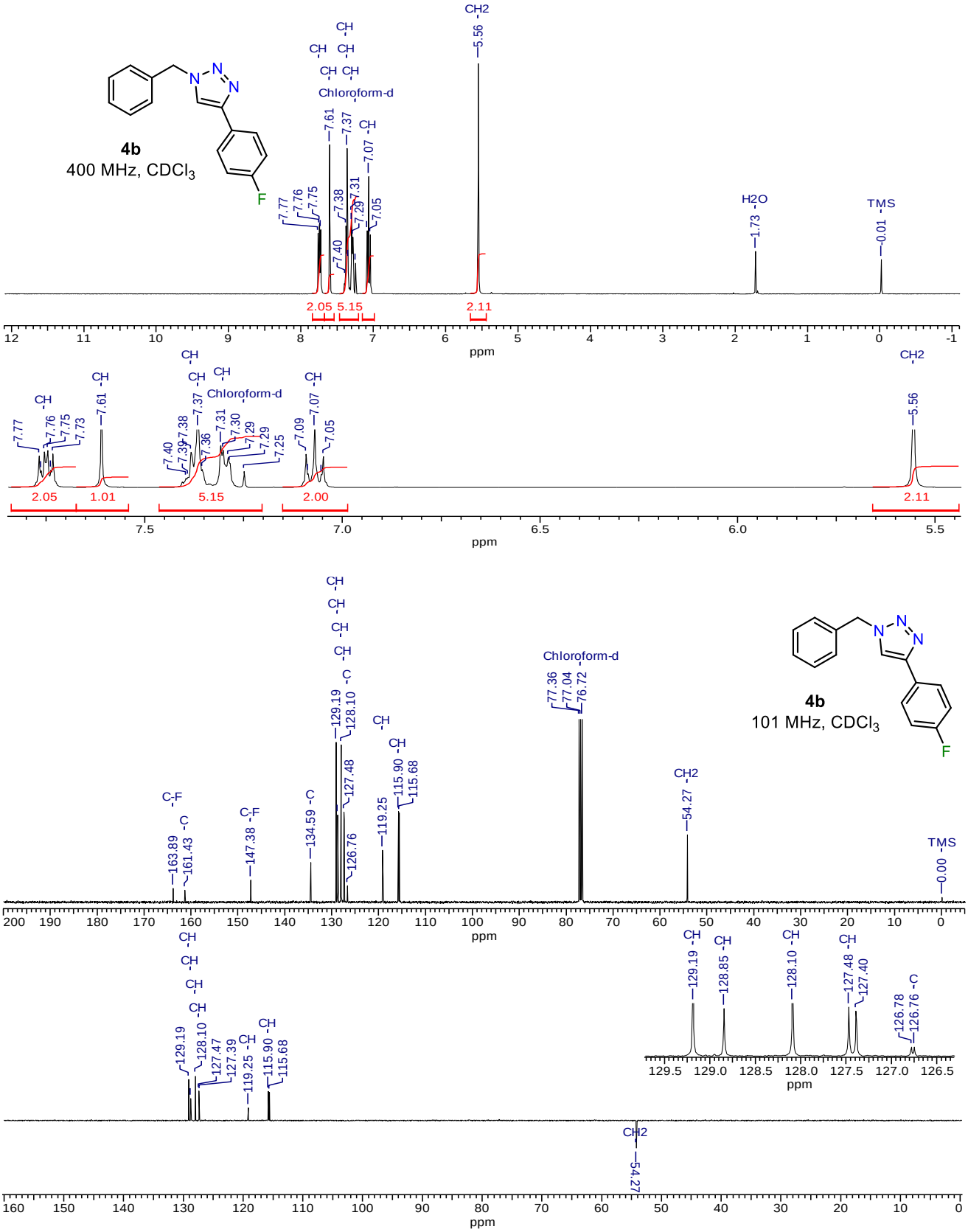

Figure S12. ^{1}H and $^{13}C\{^{1}H\}$ NMR spectra of 1-benzyl-4-(4-fluorophenyl)-1*H*-1,2,3-triazole (**4b**)

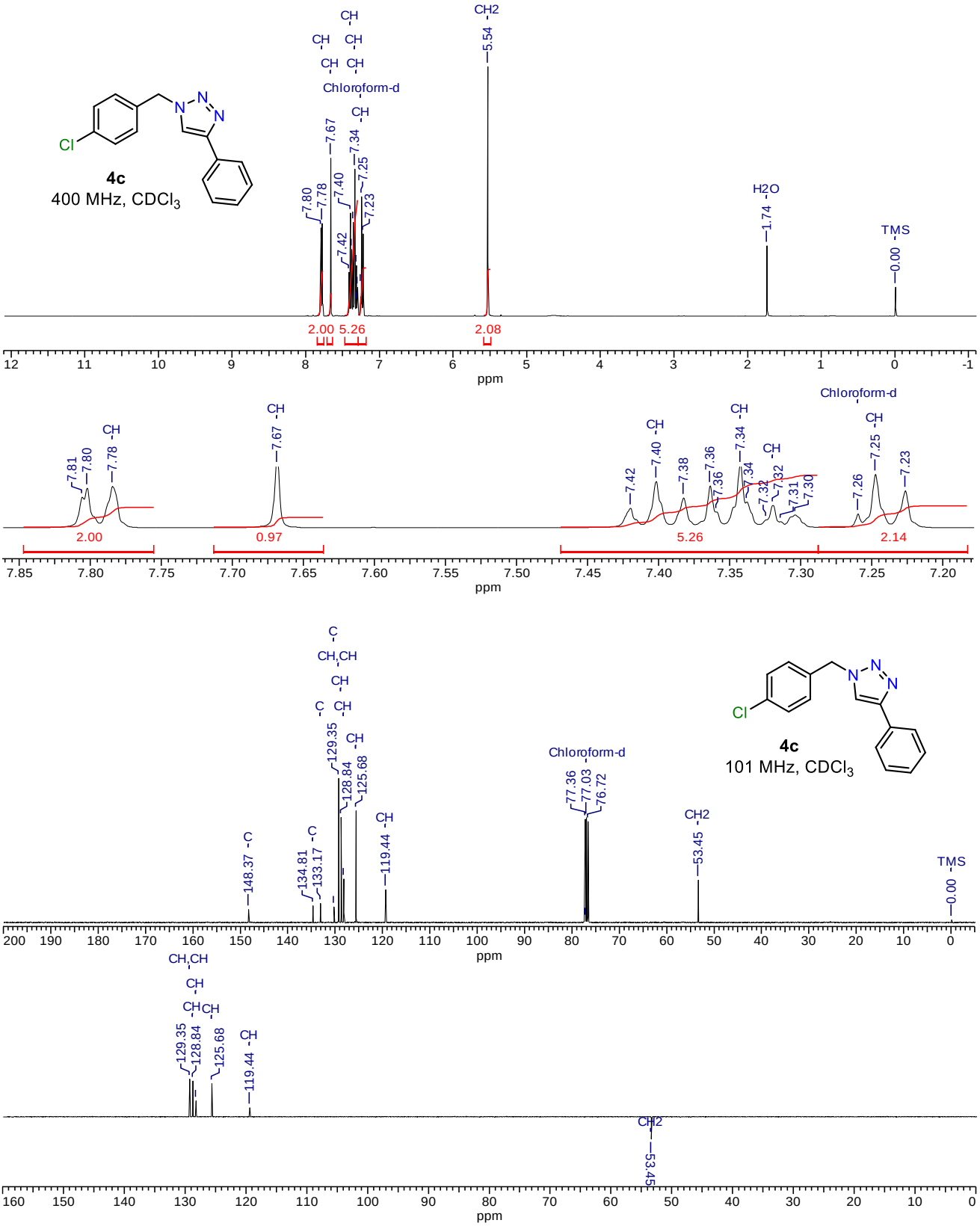

Figure S13. ^{1}H and $^{13}C\{^{1}H\}$ NMR spectra of 1-(4-chlorobenzyl)-4-phenyl-1*H*-1,2,3-triazole (**4c**)

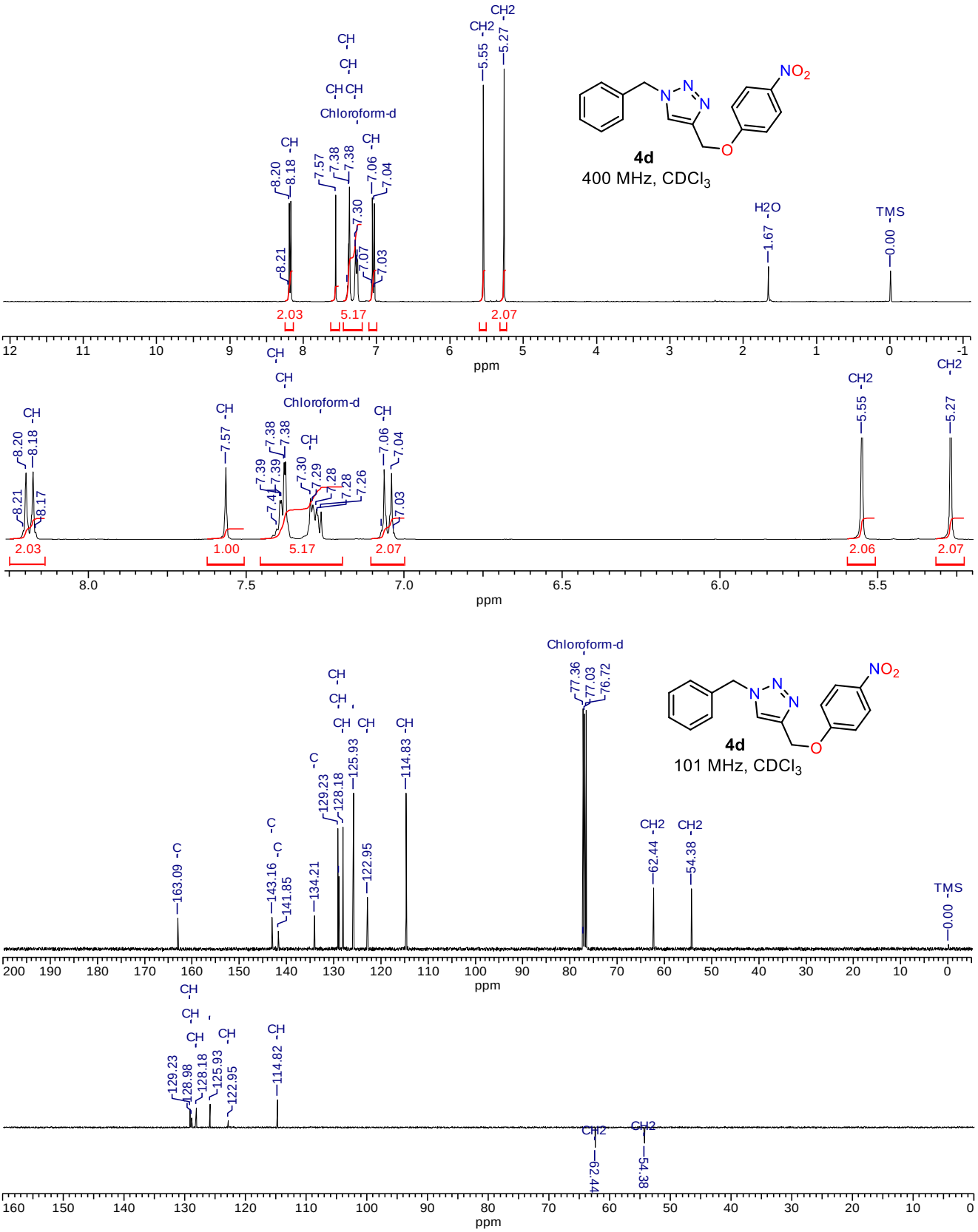

Figure S14. ^{1}H and $^{13}C\{^{1}H\}$ NMR spectra of 1-benzyl-4-((4-nitrophenoxy)methyl)-1*H*-1,2,3-triazole (**4d**)

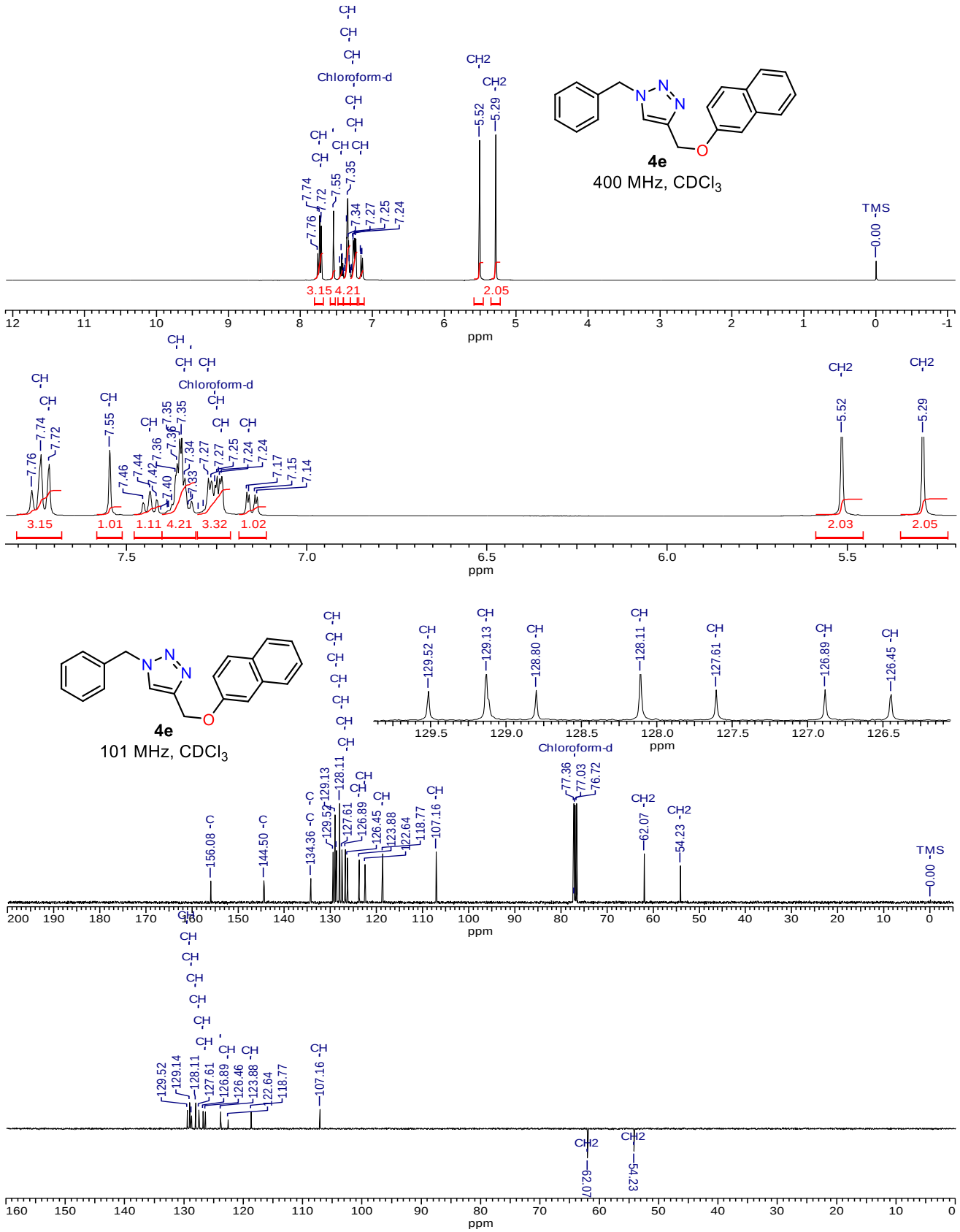

Figure S15. ^{1}H and $^{13}C\{^{1}H\}$ NMR spectra of 1-benzyl-4-((naphthalen-2-yloxy)methyl)-1*H*-1,2,3-triazole (**4e**)

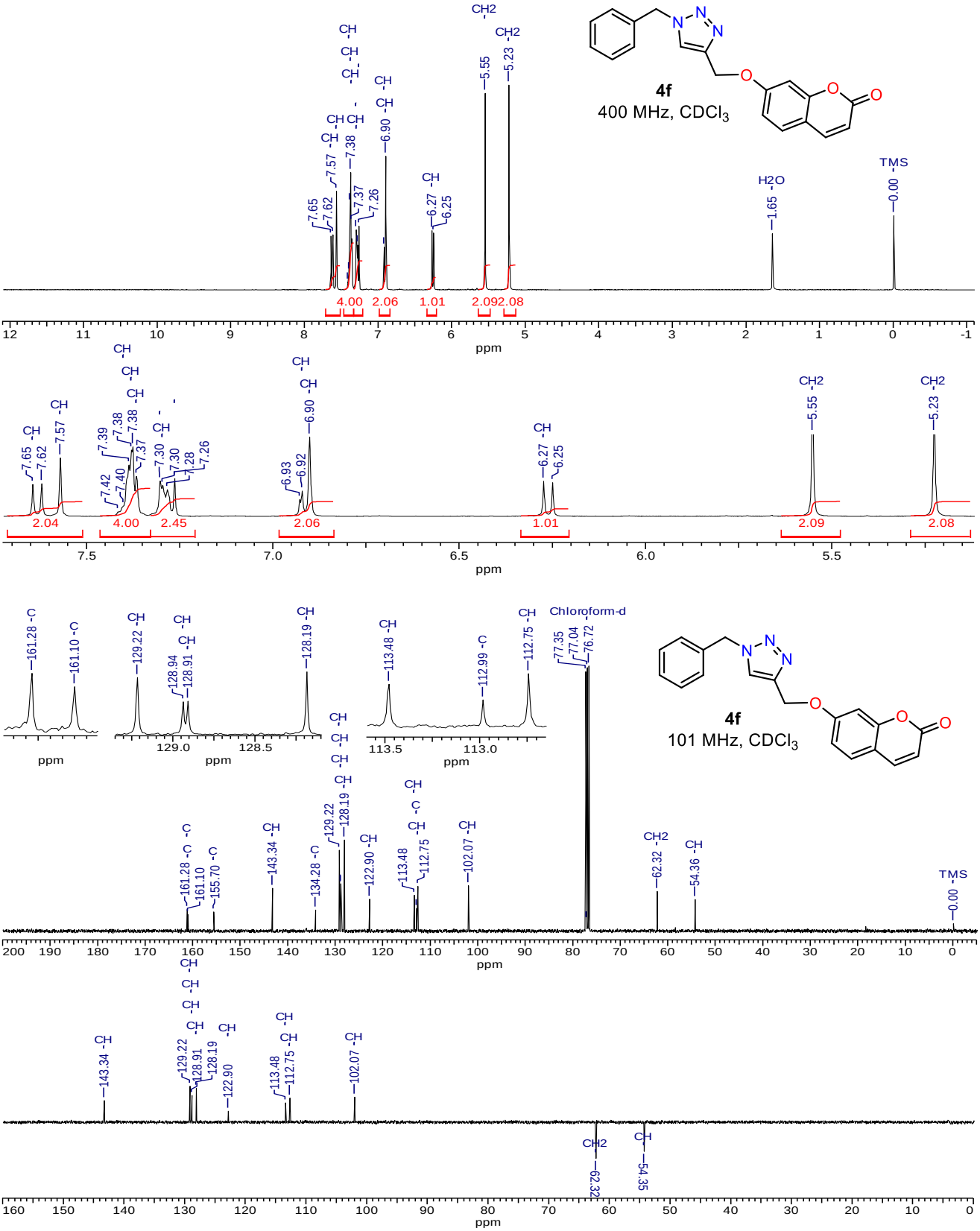

Figure S16. ^{1}H and $^{13}C\{^{1}H\}$ NMR spectra of 7-((1-benzyl-1*H*-1,2,3-triazol-4-yl)methoxy)-2*H*-chromen-2-one (**4f**)

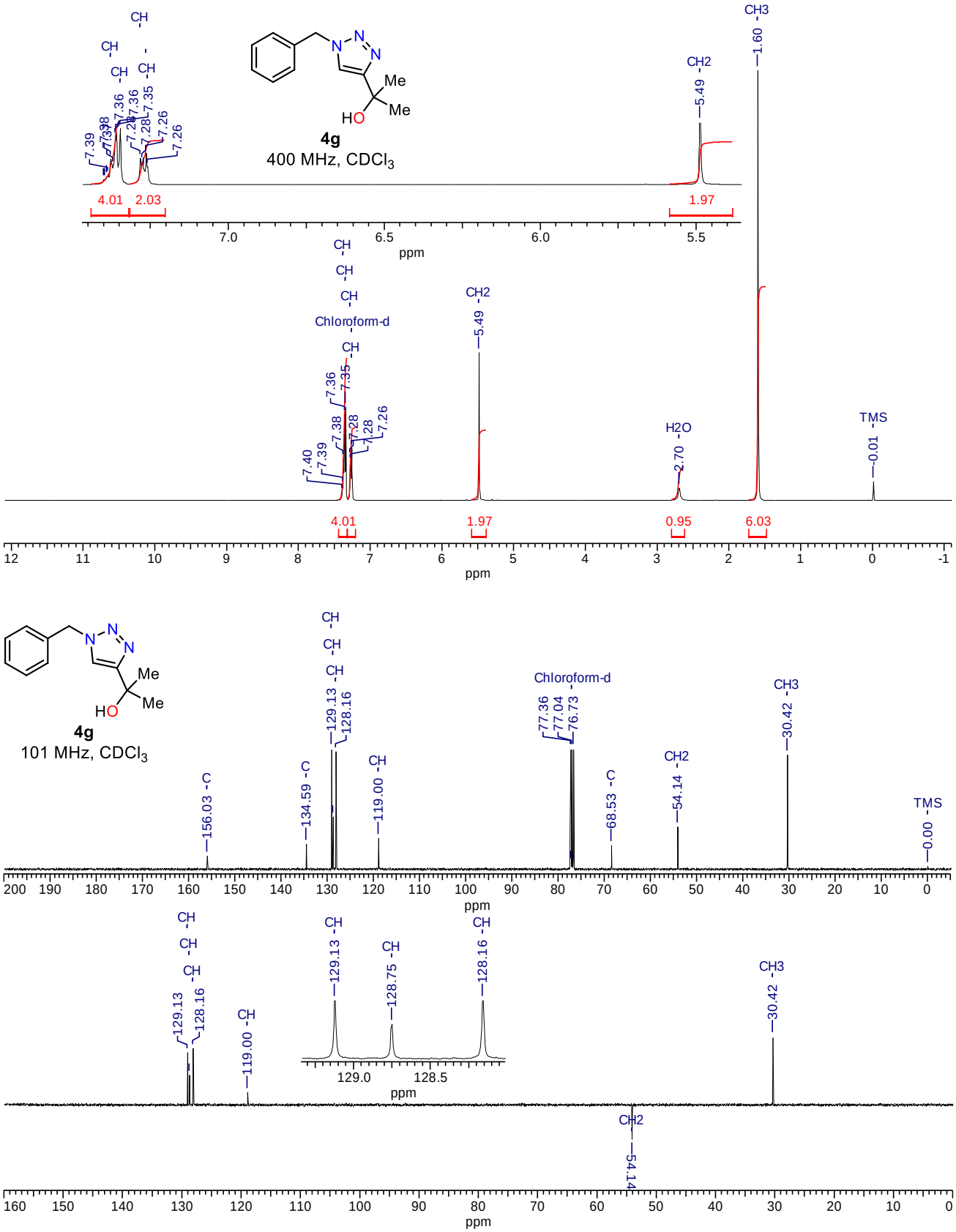

Figure S17. ^{1}H and $^{13}C\{^{1}H\}$ NMR spectra of 2-(1-benzyl-1*H*-1,2,3-triazol-4-yl)propan-2-ol (**4g**)

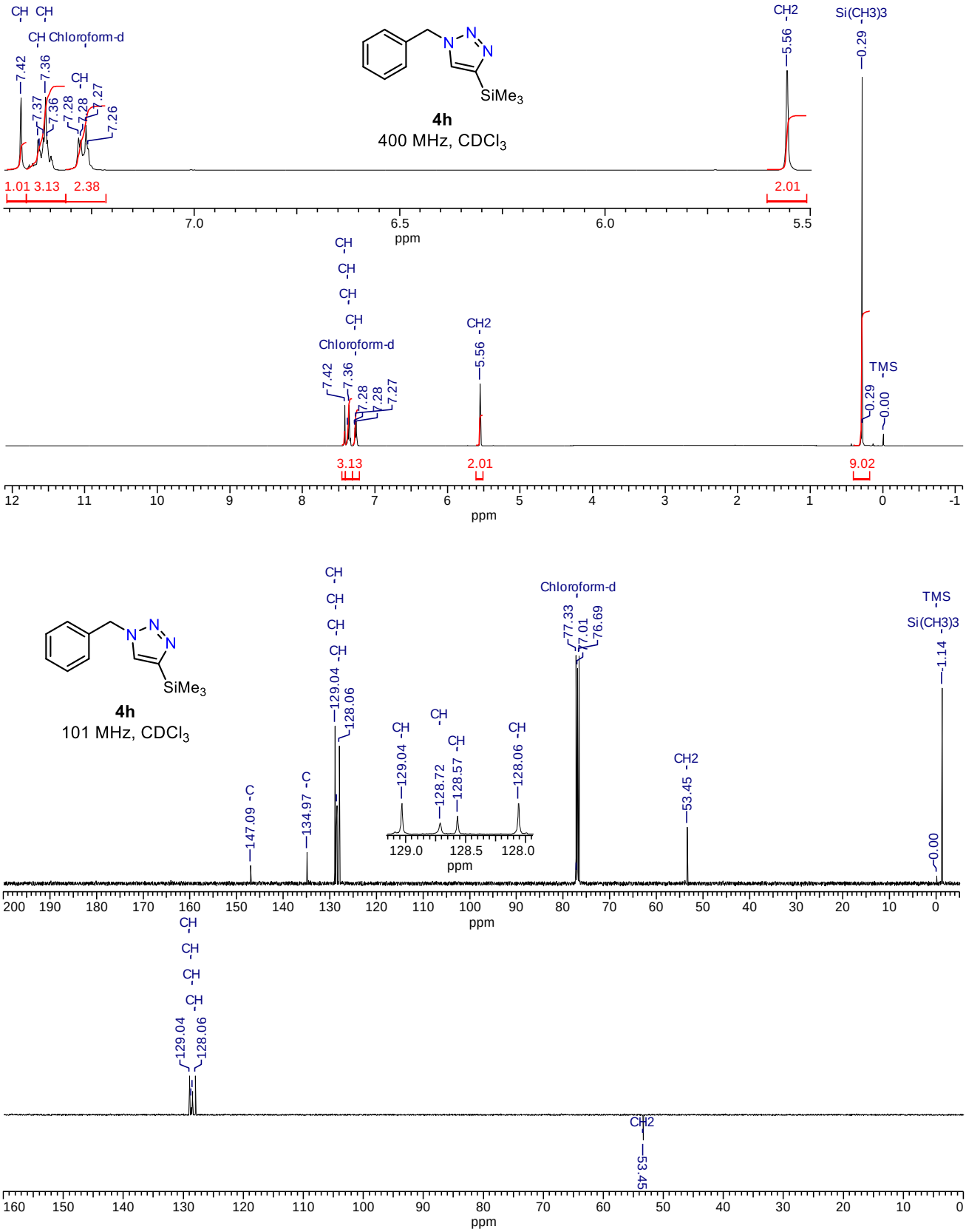

Figure S18. ^{1}H and $^{13}C\{^{1}H\}$ NMR spectra of 1-benzyl-4-(trimethylsilyl)-1*H*-1,2,3-triazole (**4h**)

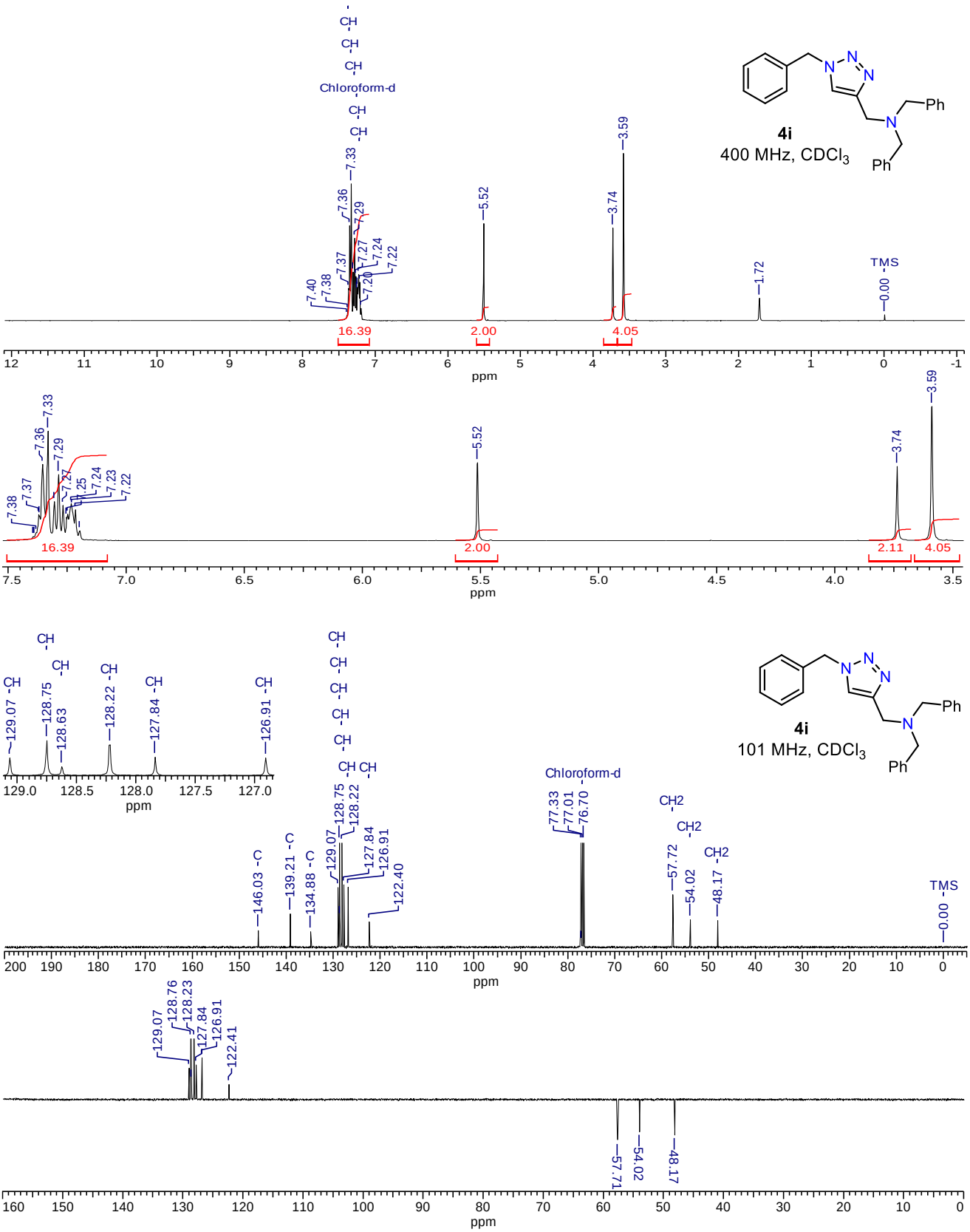

Figure S19. ^{1}H and $^{13}C\{^{1}H\}$ NMR spectra of *N*,*N*-dibenzyl-1-(1-benzyl-1*H*-1,2,3-triazol-4-yl)methanamine (**4i**)

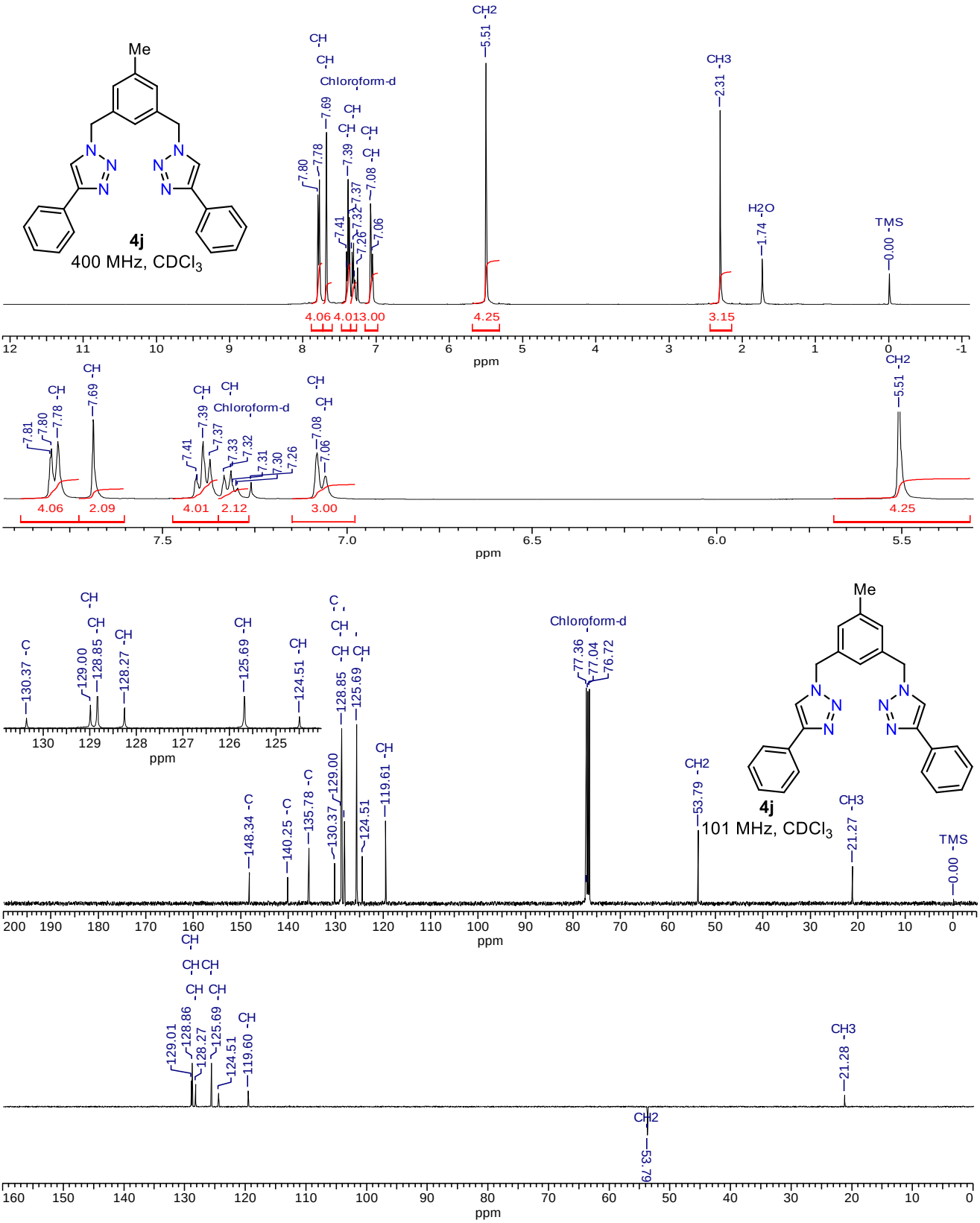

Figure S20. ^{1}H and $^{13}C\{^{1}H\}$ NMR spectra of 1,1'-((5-methyl-1,3-phenylene)*bis*(methylene))*bis*(4-phenyl-1*H*-1,2,3-triazole) (**4j**)

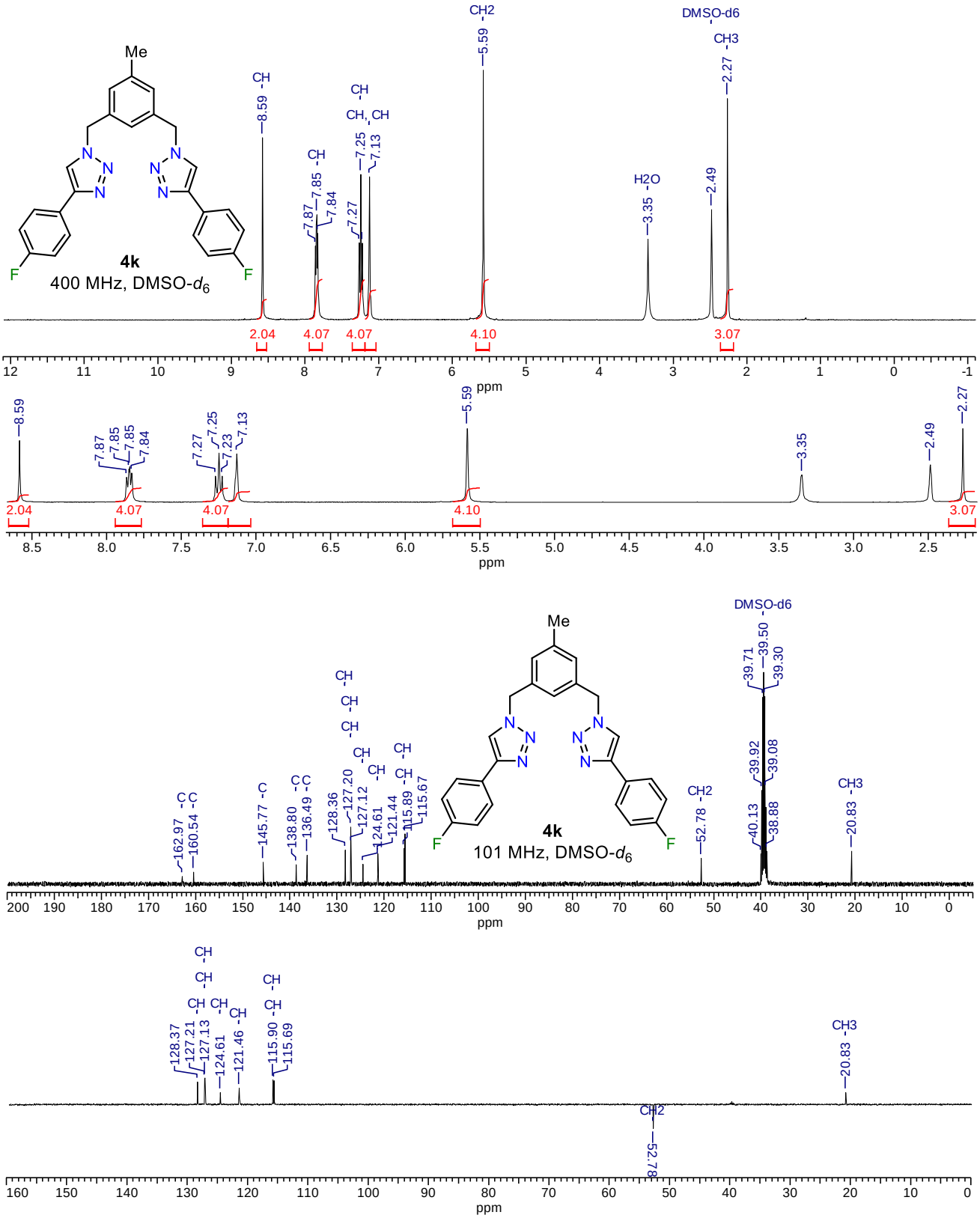

Figure S21. ^{1}H and ^{13}C{^{1}H} NMR spectra of 1,1'-((5-methyl-1,3-phenylene)*bis*(methylene))*bis*(4-(4-fluorophenyl)-1*H*-1,2,3-triazole) (**4k**)

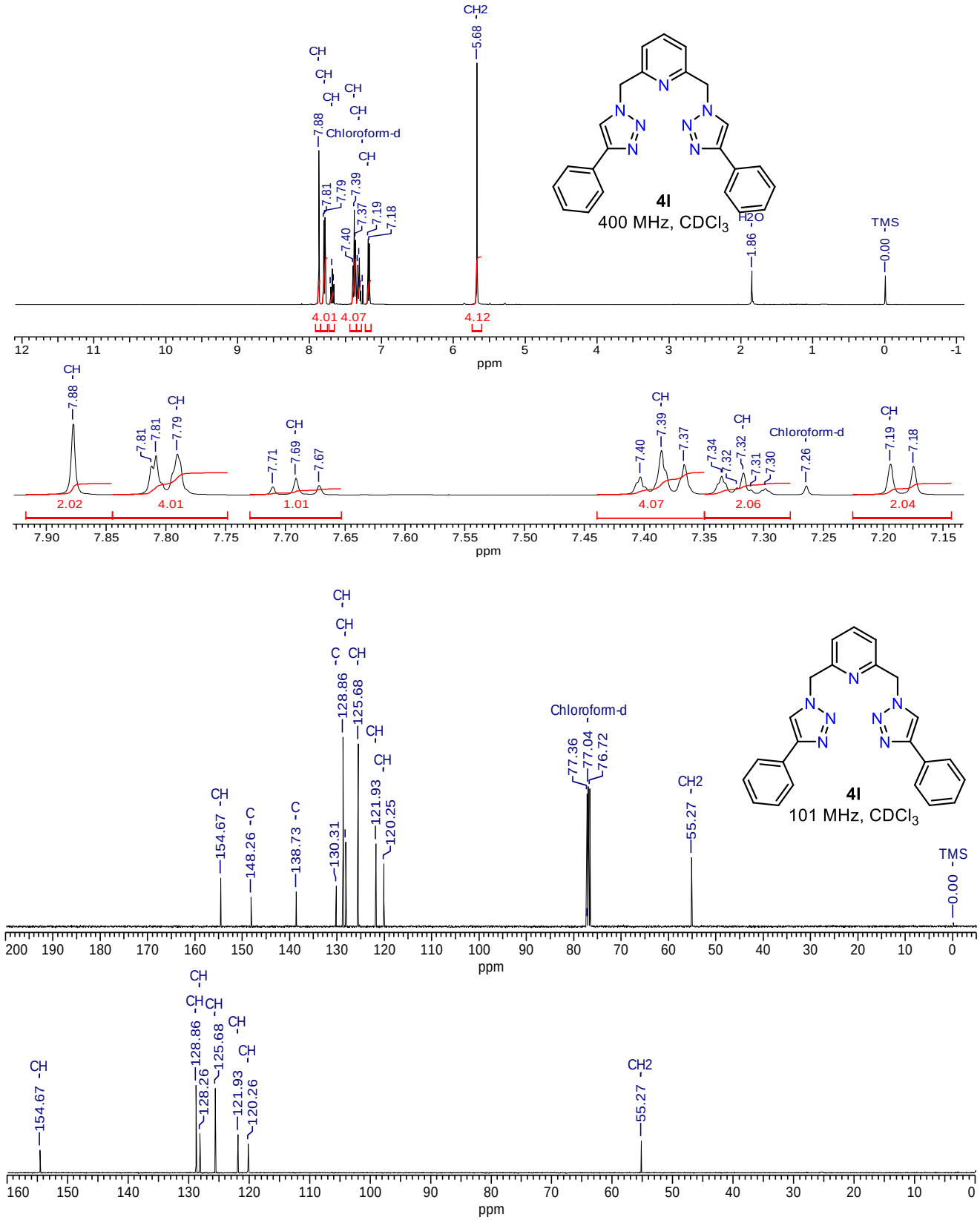

Figure S22. ^{1}H and ^{13}C{^{1}H} NMR spectra of 2,6-*bis*((4-phenyl-1*H*-1,2,3-triazol-1-yl)methyl)pyridine (**4l**)

6. References

1. Spek, A. L. PLATON SQUEEZE: a tool for the calculation of the disordered solvent contribution to the calculated structure factors. *Acta Crystallogr., Sect. C: Struct. Chem.* **2015**, *71*, 9–18.

2. Spek, A. L. Structure validation in chemical crystallography. *Acta Crystallogr., Sect. D: Struct. Biol.* **2009**, *65*, 148–155.

3. (a) Maini, L.; Braga, D.; Mazzeo, P. P.; Ventura, B. Polymorph and isomer conversion of complexes based on CuI and PPh_3 easily observed via luminescence. *Dalton Trans.* **2012**, *41*, 531–539; (b) Nuñez-Dallos, N.; Macías, M. A.; García-Beltrán, O.; Calderón, J. A.; Nagles, E.; Hurtado, J. Voltammetric determination of amaranth and tartrazine with a new double-stranded copper(I) helicate-single-walled carbon nanotube modified screen printed electrode. *J. Electroanal. Chem.* **2018**, *822*, 95–104.

4. Robinson, K. Gibbs, G. V. Ribbe, P. H. Quadratic elongation: a quantitative measure of distortion in coordination polyhedra. *Science* **1971**, *172*, 567–570.

5. Thomas, J. C.; Peters, J. C. Structural and spectroscopic studies of three-coordinate copper(I) supported by *bis*(phosphino)borate ligands. *Polyhedron* **2004**, *23*, 2901–2913.

6. Mankad, N. P.; Antholine, W. E.; Szilagyi, R. K.; Peters, J. C. Three-coordinate copper(I) amido and aminyl radical complexes. *J. Am. Chem. Soc.* **2009**, *131*, 3878–3880.

7. Kundu, S.; Greene, C.; Williams, K. D.; Salvador, T. K.; Bertke, J. A.; Cundari, T. R.; Warren, T. H. Three-coordinate copper(II) aryls: key intermediates in C–O bond formation. *J. Am. Chem. Soc.* **2017**, *139*, 9112−9115.

8. Rueda-Espinosa, J.; Torres, J. F.; Valdez Gauthier, C.; Wojtas, L.; Verma, G.; Macías, M. A.; Hurtado J. Copper(II) complexes with tridentate *bis*(pyrazolylmethyl)pyridine ligands: synthesis, X-ray crystal structures and ε-caprolactone polymerization. *ChemistrySelect* **2017**, *2*, 9815–9821.

9. Sandoval-Rojas, A. P.; Ibarra, L.; Cortés, M. T.; Hurtado, M.; Macías, M.; Hurtado, J. Synthesis and characterization of a new copper(II) polymer containing a thiocyanate bridge and its application in dopamine detection. *Inor. Chim. Acta* **2017**, *459*, 95–102.

10. Sandoval-Rojas, A. P.; Ibarra, L.; Cortés, M. T.; Macías, M. A.; Suescun L.; Hurtado, J. Synthesis and characterization of copper(II) complexes containing acetate and *N*,*N*-donor ligands, and their electrochemical behavior in dopamine detection. *J. Electroanal. Chem.* **2017**, 805, 60–67.

11. Hurtado, J.; Ibarra, L.; Yepes, D.; García-Huertas, P.; Macías, M. A.; Triana-Chavez, O.; Nagles, E.; Suescun, L.; Muñoz-Castro, A. Synthesis, crystal structure, catalytic and anti-*Trypanosoma cruzi* activity of a new chromium(III) complex containing *bis*(3,5-dimethylpyrazol-1-yl)methane. *J. Mol. Struct.* **2017**, *1146*, 365–372.

12. Torres, J. F.; Bello-Vieda, N. J.; Macías, M. A.; Muñoz-Castro, A.; Rojas-Dotti, C.; Martínez-Lillo, J.; Hurtado, J. Water dissociation of a dinuclear *bis*(3,5-dimethylpyrazolyl)methane copper(II) complex: X-ray diffraction structure, magnetic properties, and characteristic absorption of the $(CuN_2Cl_2)_2$ core. *Eur. J. Inorg. Chem.* **2018**, *32*, 3644–3651.

13. Turner, M. J.; McKinnon, J. J.; Wolff, S. K.; Grimwood, D. J.; Spackman, P. R.; Jayatilaka, D.; Spackman, M. A. (2017). *CrystalExplorer17*. University of Western Australia. http:// hirshfeldsurface.net/ .

14. (a) Parr, R. G.; Gazquez, J. L. Hardness functional. *J. Phys. Chem.* 1993, *97*, 3939–3940; (b) Schulze. B.; Schubert, U. S. Beyond click chemistry–supramolecular interactions of 1,2,3-triazoles. *Chem. Soc. Rev.* **2014**, *43*, 2522–2571; (c) Ekennia, A. C.; Osowole, A. A.; Olasunkanmi, L. O.; Onwudiwe, D. C.; Olubiyi, O. O.; Ebenso, E. E. Synthesis, characterization, DFT calculations and molecular docking studies of metal (II) complexes. *J. Mol. Struct.* **2017**, *1150*, 279–202.